Evaluation of the Therapeutic and Diagnostic Effects of PEGylated Liposome–Embedded ^{188}Re on Human Non–Small Cell Lung Cancer Using an Orthotopic Small-Animal Model

Liang-Ting Lin[1], Chih-Hsien Chang[1,2], Hsiang-Lin Yu[2], Ren-Shyan Liu[1,3–5], Hsin-Ell Wang[1,5], Shu-Jun Chiu[6,7], Fu-Du Chen[8], Te-Wei Lee[2], and Yi-Jang Lee[1,5]

[1]Department of Biomedical Imaging and Radiological Sciences, National Yang-Ming University, Taipei, Taiwan; [2]Institute of Nuclear Energy Research, Taoyuan, Taiwan; [3]Department of Nuclear Medicine, National PET/Cyclotron Center, Taipei Veterans General Hospital, Taipei, Taiwan; [4]NRPB/Taiwan Mouse Clinic/Molecular and Genetic Imaging Core, Taipei, Taiwan; [5]Biophotonics and Molecular Imaging Research Center (BMIRC), National Yang-Ming University, Taipei, Taiwan; [6]Department of Life Sciences, Tzu Chi University, Hualien, Taiwan; [7]Institute of Radiological Sciences, Tzu Chi Technology College, Hualien, Taiwan; and [8]Graduate Institute of Biotechnology, Chinese Culture University, Taipei, Taiwan

Non–small cell lung cancer (NSCLC) is a highly morbid and mortal cancer type that is difficult to eradicate using conventional chemotherapy and radiotherapy. Little is known about whether radionuclide-based pharmaceuticals can be used for treating NSCLC. Here we embedded the therapeutic radionuclide ^{188}Re in PEGylated (PEG is polyethylene glycol) liposomes and investigated the biodistribution, pharmacokinetics, and therapeutic efficacy of this nanoradiopharmaceutical on NSCLC using a xenograft lung tumor model and the reporter gene imaging techniques. **Methods:** Human NSCLC NCI-H292 cells expressing multiple reporter genes were used in this study. ^{188}Re was conjugated to *N,N*-bis(2-mercaptoethyl)-*N′,N′*-diethylethylenediamine (BMEDA) and loaded into the PEGylated liposome to form a ^{188}Re-liposome. The tumor growth rates and localizations were confirmed using bioluminescent imaging and SPECT/CT after the ^{188}Re-BMEDA or ^{188}Re-liposome was intravenously injected. The accumulation of the nanodrug in various organs was determined by the biodistribution analysis and the nano-SPECT/CT system. The pharmacokinetic and dosimetric analyses were further determined using WinNonlin and OLINDA/EXM, respectively. **Results:** The biodistribution and nano-SPECT/CT imaging showed that PEGylated ^{188}Re-liposome could efficiently accumulate in xenograft tumors formed by NCI-H292 cells that were subcutaneously implanted in nude mice. Pharmacokinetic analysis also showed that the retention of ^{188}Re-liposome was longer than that of ^{188}Re-BMEDA. In an orthotopic tumor model, ex vivo γ counting revealed that the uptake of ^{188}Re-liposome was detected in tumor lesions but not in surrounding normal lung tissues. Moreover, we evaluated the therapeutic efficacy using bioluminescent imaging and showed that the lung tumor growth was suppressed but not eradicated by ^{188}Re-liposome. The life span of ^{188}Re-liposome–treated mice was 2-fold longer than that of untreated control mice. **Conclusion:** The results of biodistribution, pharmacokinetics, estimated dosimetry, nano-SPECT/CT, and bioluminescent imaging suggest that the PEGylated liposome–embedded ^{188}Re could be used for the treatment of human lung cancers.

Key Words: NSCLC; nanoradiopharmaceuticals; ^{188}Re; SPECT/CT; pharmacokinetics

J Nucl Med 2014; 55:1864–1870
DOI: 10.2967/jnumed.114.140418

According to a 2008 World Cancer Report published by the World Health Organization, lung cancer is the leading cause of death among various types of cancers. More than 80% of human lung cancers are categorized as non–small cell lung cancer (NSCLC). Lobectomy is the major therapeutic strategy to treat NSCLC, followed by adjuvant chemotherapy or external-beam radiotherapy (*1–3*). However, advanced NSCLC exhibits a high frequency of resistance to chemotherapy and radiotherapy, suggesting that alternative approaches need to be developed for NSCLC treatment (*4–6*).

Radiopharmaceuticals are radionuclides that can be used for diagnosis or therapy of internal diseases. Different decay modes of radionuclides lead to emission of high-energy photons or charged particles for medical applications. ^{99m}Tc pharmaceuticals can emit γ rays (140 keV) that are detectable using the γ camera or a SPECT scanner for clinical diagnosis. This radionuclide can be used for imaging various organs, depending on the types of biochemical compounds that chelate to ^{99m}Tc (*7,8*). However, whether radiopharmaceuticals can provide both therapeutic and diagnostic value for human lung cancers remains to be addressed.

^{188}Re is a noteworthy therapeutic radionuclide with potential value in diagnosis because it emits both γ rays (155 keV) and an extremely high energy of β particles (2.12 MeV) during decay. Its atomic radius is similar to technetium, and both radionuclides share common chemistry (*9,10*). Moreover, the tissue penetration of emitted β particles is only 5 mm, but it is sufficient to suppress the proliferation of human cancer cells with little damage to surrounding normal tissues (*11*). However, ^{188}Re is non–tissue-specific, so that it has to be conjugated to biochemical compounds that can target tumor tissues for radionuclide-based therapy. For instance, it has been reported that conjugation of ^{188}Re to monoclonal antibodies and hydroxyethylidene diphosphonate can suppress cancer growth and relieve the pain caused by bone metastasis, respectively (*12–14*). Recently, ^{188}Re has been embedded in nanoscale liposomes via *N,N*-bis(2-mercaptoethyl)-*N′,N′*-diethylethylenediamine

Received Mar. 19, 2014; revision accepted Sep. 12, 2014.
For correspondence or reprints contact either of the following:
Te-Wei Lee, No. 1000, Wenhua Rd., Jiaan Village, Taoyuan 32546, Taiwan.
E-mail: twlee@iner.gov.tw
Yi-Jang Lee, National Yang-Min University, No. 155, Sec. 2, Li-Nong St., Beitou District, Taipei 11221, Taiwan.
E-mail: yjlee2@ym.edu.tw
Published online Oct. 27, 2014.

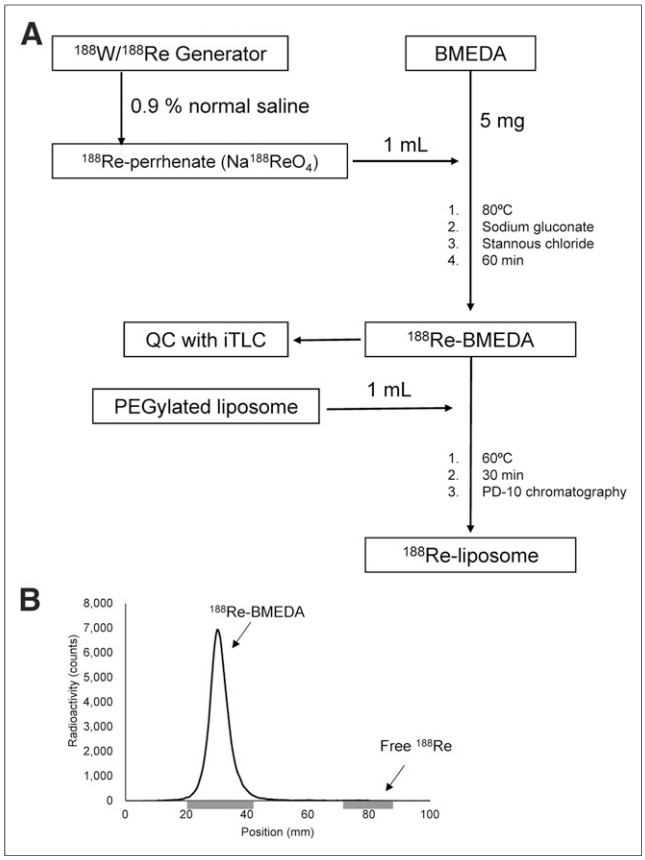

FIGURE 1. Procedures for production and quality validation of PEGylated ^{188}Re-liposome. (A) Flowchart for ^{188}Re-liposome production. (B) iTLC analysis for assessing embedding efficiency.

(BMEDA) chelator and proved to be ideal for targeting in the local and lung metastatic colorectal cancer animal model (*15*). Additionally, conjugation of ^{188}Re or ^{99m}Tc to the somatostatin receptor–binding peptide analog P2045 has been demonstrated to be a potent radiopharmaceutical for lung cancer therapy and diagnosis, and it has entered phase I clinical trials (*16–18*). Whether ^{188}Re conjugated to nanoscale liposomes is also beneficial for the treatment of human NSCLC would be of interest to investigate further.

In this study, we embedded ^{188}Re-BMEDA in PEGylated (PEG is polyethylene glycol) liposomal particles for the treatment of human NSCLC in the xenograft tumor model. The pharmacokinetics and the absorbed dose estimation of ^{188}Re-liposome administration were revealed by SPECT/CT imaging and biodistribution analysis. The current results demonstrated that the ^{188}Re-liposome exhibited longer retention and better tumorous accumulation than ^{188}Re-BMEDA in vivo. The results of bioluminescent imaging (BLI) showed that tumor growth was suppressed, but not eradicated, by ^{188}Re-liposome, and the survival rate of treated tumor-bearing mice was higher than that of mock-treated control mice. Taken together, the current data suggest that use of ^{188}Re-liposome for lung cancer treatment would be a potent clinical application.

MATERIALS AND METHODS

Cell Lines

Human NSCLC NCI-H292 cells (Bioresource Collection and Research Center) were maintained in RPMI-1640 (Invitrogen Inc.) with a supplement of 10% fetal bovine serum (ThermoFisher Scientific Inc.). To produce lentiviral particles, 293T cells were cultured in Dulbecco modified Eagle medium with the 10% fetal bovine serum supplied. Cells were incubated at 37°C in a humidified incubator containing 5% CO_2.

Polycistronic Plasmid and Lentiviral Infection of Reporter Genes

The LT-3R polycistronic lentiviral plasmid, which has constitutive expression of green fluorescent protein, firefly luciferase, and herpes simplex virus type I thymidine kinase (HSV1-tk), was constructed and produced as previously described (*19*). The infected cells were subjected to fluorescence-activated cell sorting (FACSAria; BD Biosciences) for isolation of stably expressing cells.

Establishment of Tumor-Bearing Animal Model

The stable cell line with multiple reporters, named H292-GLT, was inoculated on nude mice with subcutaneous or orthotopic injection. For subcutaneous implantation, 5×10^6 cells were suspended in OPTI-MEM (Invitrogen Inc.) and mixed with Matrigel Matrix High Concentration (#354248; BD Biosciences) and then injected into the left hind limb of nude mice. For orthotopic inoculation, a 1-cm incision was made on the left chest wall of nude mice to precisely locate the insertion of the needle, and 10^6 H292-GLT cells were injected through a 29-gauge syringe in a mixture with Matrigel. The size of the subcutaneous tumor (mm^3) was calculated as $[\text{width}^2 \times \text{length}]/2$ (*20*). All the experimental animals were housed and cared for by following the standard protocols laid out by the National Laboratory Animal Center and approved by the Institutional Animal Care and Use Committee (IACUC) of National Yang-Ming University.

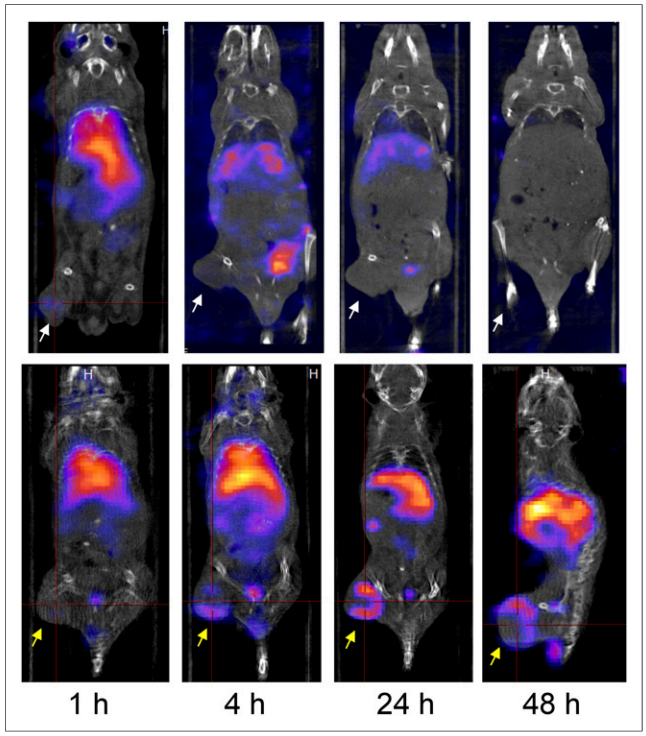

FIGURE 2. Nano-SPECT/CT imaging of ^{188}Re-BMEDA and ^{188}Re-liposome distribution in NCI-H292 tumor–bearing mice. Tumors were implanted into left hind limb of each nude mouse ($n = 3$). After intravenous injection of ^{188}Re-BMEDA (upper) and ^{188}Re-liposome (lower), nano-SPECT/CT imaging was acquired at 1, 4, 24, and 48 h. Arrows indicate positions of subcutaneous tumors with or without radioactive signals.

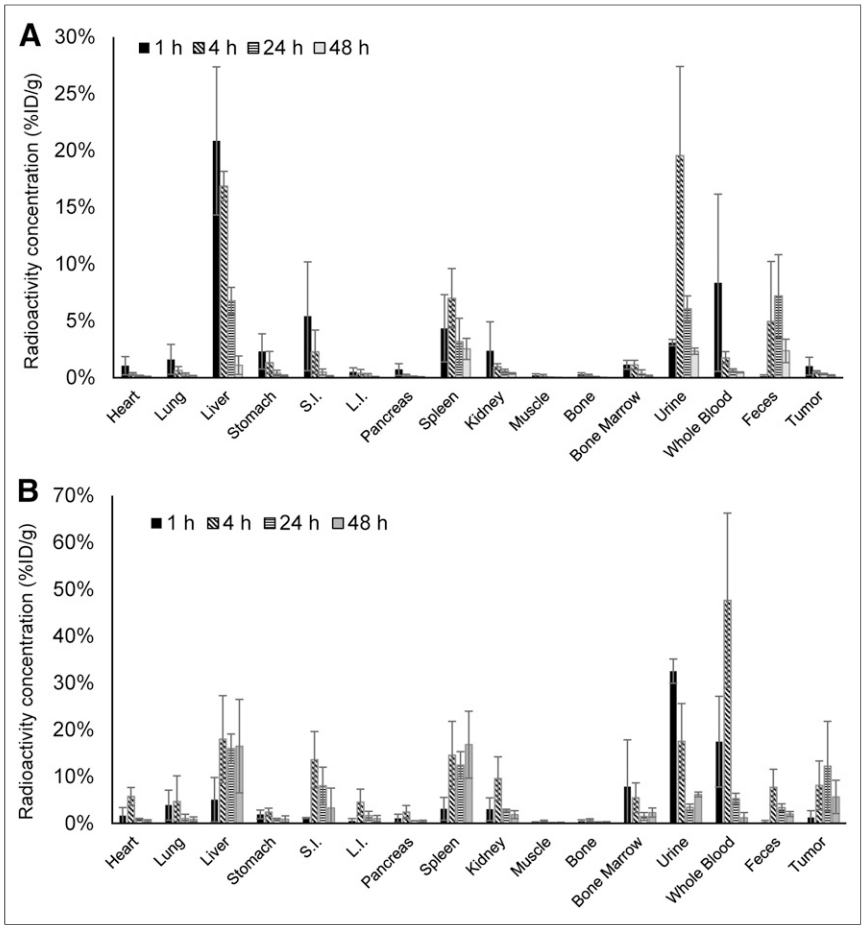

FIGURE 3. Biodistribution analysis of ^{188}Re-BMEDA and ^{188}Re-liposome in tumor-bearing mice. (A) Results of ^{188}Re-BMEDA. (B) Results of ^{188}Re-liposome. Radioactivity in each organ is demonstrated by bar charts (n = 5). L.I. = large intestine; S.I. = small intestine.

Preparation of ^{188}Re-BMEDA and ^{188}Re-Liposome

The procedure to prepare the radioactive material–embedded liposome was previously described (*21,22*) and is illustrated in Figure 1A. Briefly, ^{188}Re was milked from a ^{188}W/^{188}Re generator (Institut National des Radioelements, Fleurus, Belgium) (*23*). The eluted sodium perrhenate ($Na^{188}ReO_4$) was conjugated with BMEDA (ABX GmbH) by an hour of incubation in an 80°C water bath. The PEGylated liposome (phospholipids [13.16 μmol/mL]) (NanoX; Taiwan Liposome Co. Ltd.) was added into the ^{188}Re-BMEDA solution for another 30-min incubation in a 60°C water bath. Labeling of ^{188}Re-BMEDA was tested by instant thin-layer chromatography (iTLC) using a radio–thin-layer chromatography scanner (Bioscan AR2000; Bioscan, TriFoil Imaging Inc.). The embedded liposome was isolated from free ^{188}Re-BMEDA by PD-10 chromatographic column (GE Healthcare) elution. The liposomal loading efficiency (%) of ^{188}Re-liposome was calculated as

$$\frac{\text{Total radioactivity eluted}}{\text{Remnant radioactivity in chromatographic column}}. \quad \text{(Eq. 1)}$$

Biodistribution and Pharmacokinetic Analysis

Forty lung cancer–bearing mice (5 mice per group for each time point) were intravenously injected with ^{188}Re-BMEDA or ^{188}Re-liposome (1.85 MBq/100 μL). After certain times (1, 4, 24, and 48 h), the mice were sacrificed by CO_2 asphyxiation for the collection of samples. Each collected organ was weighed and counted by a γ counter (Cobra II Auto-Gamma Counter; PerkinElmer Inc.), and the results were presented as percentage injected dose per gram. For pharmacokinetic analysis, the tumor-bearing mice were injected with ^{188}Re-BMEDA or ^{188}Re-liposome (1.85 MBq/100 μL). The blood samples were collected by tail vein puncture with microliter capillary tubes at different times, including 0.083, 0.25, 0.5, 1, 2, 4, 8, 16, 24, and 48 h. The samples were counted and calculated by Pharsight WinNonlin 5.2 software (Certara L.P.).

Dosimetric Evaluation of ^{188}Re-Liposome Absorbed Radiation Dose In Vivo

To estimate the internal absorbed radiation dose in humans, we extrapolated the calculated mean value of percentage injected dose per weighed unit (g) from mice to humans. The dissected organs were weighed and counted from different time points, and these data were input into OLINDA/EXM software following the guidelines of MIRD pamphlets and previous studies (*24,25*) to calculate dose estimates.

In Vivo Radionuclide-Based Imaging and BLI

To track tumor growth with multiple imaging probes, ^{123}I-1-(2-deoxy-2-fluoro-1-D-arabinofuranosyl)-5-iodouracil (^{123}I-FIAU) was prepared as previously described (*26*). Tumor-bearing mice were fed with 0.5% v/v Lugol iodine drinking water 1 h before the ^{123}I-FIAU administration. Ten hours after intravenous ^{123}I-FIAU injection, the mice were imaged using the nano-SPECT/CT scanner (Mediso Ltd.). To monitor and quantify tumor growth in the orthotopic tumor–bearing model, mice were injected with D-luciferin (150 mg/kg) (VivoGlo Luciferin; Promega Corp.) intraperitoneally. The In Vivo Imaging System 50 (Perkin Elmer Inc.) was used for BLI. All imaged mice were anesthetized by 1% isoflurane inhalation and warmed until they awakened.

Statistical Analysis

The results demonstrated in this study were analyzed by the Student t test, with a P value of less than 0.05 indicating a significant

TABLE 1
Pharmacokinetic Analysis in Human NSCLC–Bearing Mice

Parameter	Unit	^{188}Re-BMEDA	^{188}Re-liposome
C_{max}	%ID/mL	7.40	39.72
Cl	mL/h	1.61 ± 0.18	0.21 ± 0.02
$AUC_{(0\to\infty)}$	h·%ID/mL	62.73 ± 7.26	488.97 ± 52.83
$MRT_{(0\to\infty)}$	hours	5.07 ± 3.39	13.04 ± 4.32

C_{max} = larger maximal concentration; %ID = percentage injected dose; Cl = clearance; $AUC_{(0\to\infty)}$ = area under curve; $MRT_{(0\to\infty)}$ = mean residence time.

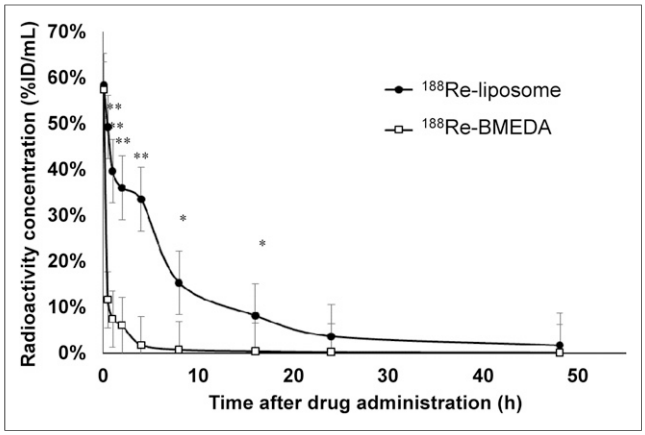

FIGURE 4. Pharmacokinetic time–activity curves in systemic circulation from tumor-bearing mice injected with either ^{188}Re-BMEDA or ^{188}Re-liposome at 0.083, 0.25, 0.5, 1, 2, 4, 8, 16, 24, and 48 h (n = 6). *$P < 0.05$. **$P < 0.01$).

difference. The Kaplan–Meier plot was generated using the MedCalc (MedCalc Software) integrated program.

RESULTS

Manufacturing Procedures and Quality Validation of ^{188}Re-BMEDA and ^{188}Re-Liposome

Conjugation of BMEDA to rhenium perrhenate ($Na^{188}ReO4$) is required for the production of ^{188}Re-liposome, and the labeling efficiency was greater than 99% (n = 5). The manufacturing procedures of the ^{188}Re-liposome are illustrated in Figure 1A. The iTLC distinguished the free and BMEDA-labeled ^{188}Re from molecular weight shifting (Fig. 1B). The mean loading efficiency of ^{188}Re into PEGylated liposome was 71.1%, which is consistent with a previous report (*22*). Additionally, the size and surface charge of ^{188}Re-liposome were 84.6 ± 4.12 nm and 1.1 ± 1.9 mV, respectively, as measured by dynamic light scattering analysis.

Analysis of ^{188}Re-Liposomal Biodistribution in Xenograft Lung Cancer Model

We next investigated whether ^{188}Re-liposome could be used for detecting the tumor lesions in vivo. Human NSCLC H292-GLT cells were subcutaneously inoculated into the left hind limbs of nude mice. After the tumors reached 300 mm^3, the tumor-bearing mice were separated to 2 groups and intravenously injected with either ^{188}Re-BMEDA or PEGylated ^{188}Re-liposome. The mice were subsequently subjected to nano-SPECT/CT at different times up to 48 h. The results showed that both ^{188}Re-BMEDA and ^{188}Re-liposome were rapidly detected (at 1 h) after they were injected into mice. However, ^{188}Re-BMEDA was quickly washed out in tumor-bearing mice, whereas accumulation of PEGylated ^{188}Re-liposome at the tumor site remained detectable up to 48 h (Fig. 2). Therefore, these results demonstrated that ^{188}Re-liposome exhibited high retention and tumor targeting in vivo. Additionally, the quantitative biodistribution analysis of ^{188}Re-BMEDA and ^{188}Re-liposome showed that the distribution of these 2 radiopharmaceuticals at different times was distinct in several organs, including the liver, whole blood, spleen, and tumors. Rapid washout was observed in ^{188}Re-BMEDA (Fig. 3).

Pharmacokinetic Analysis of PEGylated ^{188}Re-Liposome

We further analyzed the pharmacokinetic curves of ^{188}Re-BMEDA and PEGylated ^{188}Re-liposome in vivo. Compared with ^{188}Re-BMEDA, ^{188}Re-liposome exhibited a long mean residence time, larger maximal concentration, and a slow pace of clearance (Table 1; Fig. 4). The area under the curve calculated from the time–activity curve showed that the liposomal encapsulation avoided rapid excretion and extended the mean residence time, suggesting that the enhanced permeability and retention effect was effective in this PEGylated radiopharmaceutical application. Moreover, we estimated the radiation dose in humans according to the results of murine biodistribution and determined that the absorbed dose ratio of tumor to lung could be up to 380.7-fold (within a 100-g tumor mass) (Table 2).

Detection of ^{188}Re-Liposome Accumulation in Established Orthotopic Lung Cancer Model

To evaluate the therapeutic efficacy of ^{188}Re-liposome, a multiple-reporter-gene–integrated orthotopic tumor-bearing animal model was established. Tumor growth can be noninvasively monitored using BLI or radionuclide-based imaging in a small-animal model (Supplemental Fig. 1; supplemental materials are available at http://jnm.snmjournals.org). First, the location of the implanted tumor in the pulmonary parenchyma was confirmed using ^{123}I-FIAU, which can be trapped by expressed HSV1-tk (Fig. 5A). The lungs dissected from the tumor-bearing mice also showed apparent bioluminescent signals that were detected in the left but not in the right lung (Fig. 5B). Using this model, we intravenously injected the PEGylated ^{188}Re-liposome to detect the accumulation of ^{123}I-FIAU in tumor-bearing mice. However, no apparent photon signals could be detected in the orthotopic lung tumor using nano-SPECT/CT (Supplemental Fig. 2). Therefore, we performed a biodistribution analysis in the orthotopic tumor model including the dissection of lung tissues from tumor-bearing mice and compared the data with normal mice. Using the γ counter, we found 56% increased uptake of ^{188}Re-liposome in the tumor-bearing lungs, compared with tumor-free lungs (Fig. 5C; Supplemental Fig. 3). Additionally, fewer CD31-expressing vasculatures were observed in the orthotopic tumor model than in subcutaneous models (Fig. 5D; Supplemental Fig. 4). Therefore, these results implied that PEGylated ^{188}Re-liposome could still accumulate in the orthotopic lung tumor.

Comparison of Therapeutic Efficacy of ^{188}Re-BMEDA and ^{188}Re-Liposome Using Orthotopic Lung Cancer Model

The ^{188}Re-BMEDA and ^{188}Re-liposome were separately injected intravenously into tumor-bearing mice with 23.68 MBq (640 μCi), the 80% maximum tolerated dose, within a single dose. BLI was used to monitor tumor growth in the thoracic cavity through the detection of luciferase activity at a fixed time interval (Fig. 6A).

TABLE 2
Tumor-to-Nontumor Ratio of Absorbed Dose Estimation

Ratio	100-g tumor mass	300-g tumor mass
Tumor to lung	380.7	129.39
Tumor to heart	12.76	4.34
Tumor to red marrow	89.86	30.54

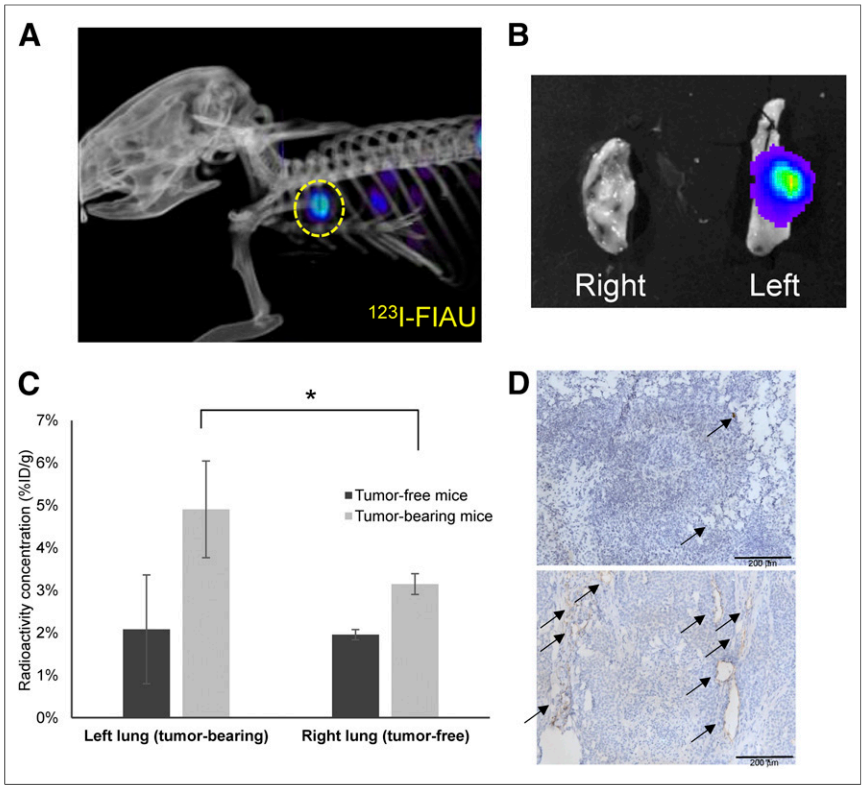

FIGURE 5. Detection of ^{188}Re-liposome distribution in orthotopic model using HSV1-tk and luciferase dual reporter genes. (A) H292-GLT cells forming orthotopic tumor were localized by administration of ^{123}I-FIAU and monitored by nano-SPECT/CT. Circle indicates location of tumor. (B) BLI was used to confirm formation of tumor in left lung of nude mouse. (C) Ex vivo tissues were subjected to γ counter for quantification. Significant difference between tumor-inoculated and non–tumor-inoculated mice was revealed. (D) Platelet endothelial cell adhesion molecule (PECAM-1) immunohistochemistry pathologic section showed that plenty of vasculature surrounded by PECAM-1 expression was observed in subcutaneous (lower) compared with orthotopic (upper) tumor. Arrows indicate PECAM-1–positive area. *$P < 0.05$.

Bioluminescent signal correlates to tumor volume (Supplemental Fig. 1). After injection, the tumor growth was monitored up to 21 d, and the results showed that ^{188}Re-liposome but not ^{188}Re-BMEDA could suppress tumor growth (Fig. 6B). Quantification of the photon flux of orthotopic lung tumors further demonstrated that tumor viability was suppressed by ^{188}Re-liposome but not by ^{188}Re-BMEDA (Fig. 6C). However, it appeared that ^{188}Re-liposome could not eradicate tumors but prevent their proliferation. Even so, the median survival time was longer in ^{188}Re-liposome–treated tumor-bearing mice than in ^{188}Re-BMEDA–treated ones (Table 3), and the Kaplan–Meier survival curves exhibited a significant difference between these 2 groups (Fig. 6D). Therefore, PEGylated ^{188}Re-liposome could suppress lung tumor growth and extend life span in the orthotopic lung tumor model.

DISCUSSION

Little is known about whether ^{188}Re-embedded liposomal drugs can be used for treatment of tumor types above the diaphragm. Here we used PEGylated ^{188}Re-liposomes to investigate their therapeutic effects on human lung cancer and showed that ^{188}Re-based radiopharmaceuticals could be applied to this cancer type.

Good targeting of cancers is one of the most important considerations in using radiopharmaceuticals for cancer treatment. However, most of the metallic radioisotopes require chemical chelators for further encapsulation into physiologically compatible vehicles, such as liposomes. In this study, the labeling efficiency of BMEDA (>99%) to ^{188}Re and the resultant radiochemical purity (>99%) were both similar to previous results (*22*), but the loading efficiency of ^{188}Re to liposome was slightly lower (71.1% ± 7.61%) than that of the previous report (82.3% ± 4.5%) (*22*).

Although the circulation period of PEGylated ^{188}Re-liposome is extended in vivo for better therapeutic efficacy, accumulation of ^{188}Re in the liver and spleen is also increased. This phenomenon may cause potent side effects (*15,22,27*). Indeed, our biodistribution study revealed that accumulation of ^{188}Re-liposome in the liver and spleen could remain up to 48 h, but ^{188}Re-BMEDA washed out after 24 h of administration. Besides, the pharmacokinetic analysis also showed that the area under the curve of ^{188}Re-liposome was 8.33-fold higher than that of ^{188}Re-BMEDA, which is comparable to another report (*28*). The maximal absorbed dose to the liver and spleen was estimated at 4.07 and 17.4 Sv, respectively, after PEGylated ^{188}Re-liposome treatment (see the "Materials and Methods" section). According to previous reports, the pathogenic dose to the liver and spleen is approximately 30 Sv (*29*). Thus, it seems that accumulation of ^{188}Re-liposome in the liver and spleen would not result in severe radiation damage. Additionally, the estimated absorbed dose was 69.86 Gy in the subcutaneous tumor (300 mm^3). Compared with the conventional clinical radiotherapeutic modality, the total tumor-absorbed dose of fractionation radiotherapy is from 60 to 80 Gy (*30*), which is comparable to the calculated radiation dose in the ^{188}Re-liposome–treated tumors. However, further investigation is necessary to determine the safety of ^{188}Re-liposome for clinical application.

One of the primary difficulties of this study was to establish an orthotopic xenograft model to mimic NSCLC in the thoracic cavity and to detect accumulation of PEGylated ^{188}Re-liposome in the tumor lesion. Because subcutaneously implanted H292-GLT tumors exhibited significant uptake of ^{188}Re-liposome, the orthotopic model is expected to have a similar result. Nevertheless, ^{188}Re-liposome in the orthotopic tumor was barely detected using nano-SPECT/CT. The maximum tumor volume implanted in the pulmonary parenchyma was around 50 mm^3, far smaller than the size of subcutaneously implanted tumors. Additionally, the emitted γ rays from ^{188}Re are only 15% of overall radioactive decay, so that the partial-volume effect resulting from the instrumental limitation may also hamper tumor detection in the orthotopic model. Using the γ-counter measurement, however, we did find that the tumor-bearing lung exhibited higher radioactivity than the normal lung in mice treated with ^{188}Re-liposome,

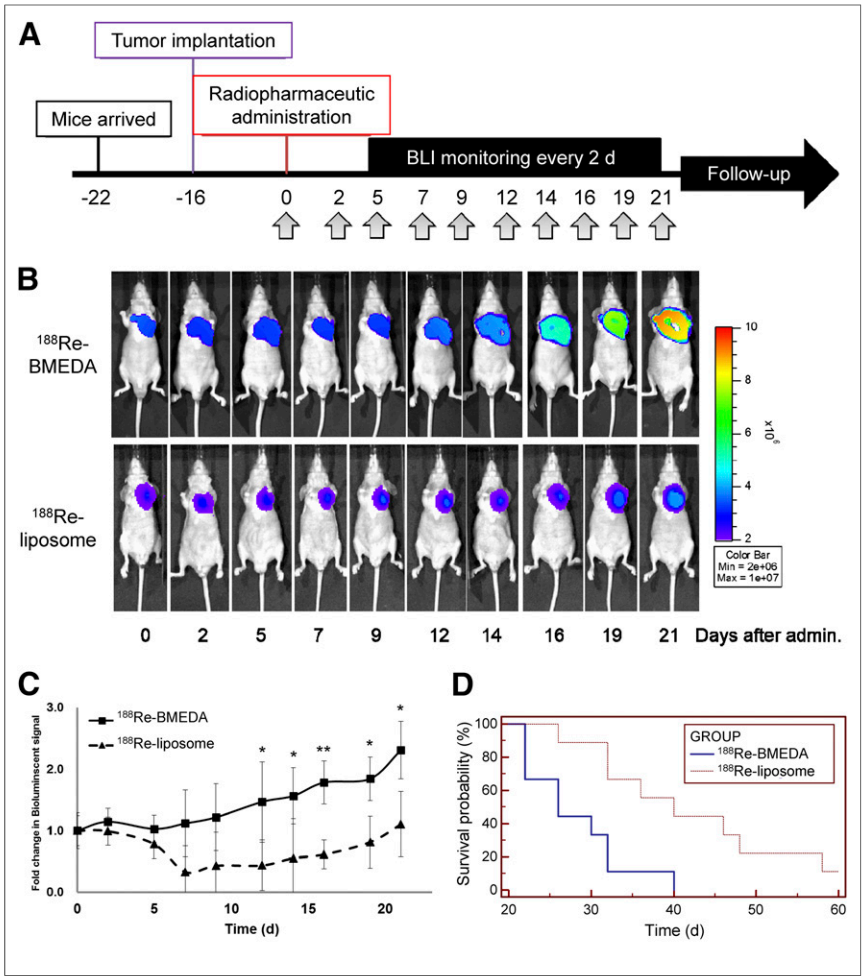

FIGURE 6. Comparison of therapeutic efficacy between ^{188}Re-BMEDA and ^{188}Re-liposome. (A) Therapeutic strategy of ^{188}Re-BMEDA or ^{188}Re-liposome. BLI was acquired at 10 time points up to 21 d. All animals were housed during this period until they reached endpoint (deceased or loss of 30% weight). (B) Bioluminescent images of orthotopic tumor growth. (C) Regions of interest quantified using LivingImage software (PerkinElmer Inc.). (D) Kaplan–Meier survival curve, with statistical analysis performed by log-rank test. *$P < 0.05$. **$P < 0.01$. admin. = administration; max = maximum; min = minimum.

suggesting that this radiopharmaceutical compound might be taken up by the orthotopic NSCLC model.

It has been reported that the administration of ^{188}Re in murine colorectal cancer and human prostate cancer models could lead to significant tumor-killing effects and extend the survival of the animals through the emitted β particles (*11,15,31*). Although we have demonstrated that the life span of tumor-bearing mice was extended by PEGylated ^{188}Re-liposome, the BLI data showed that the orthotopic lung tumors were not eradicated but their growth was suppressed. This observation may be consistent with the finding that the moderate accumulation of ^{188}Re-liposome in orthotopic lung cancer cells was not sufficient to cause tumor death but did suppress tumor growth. Several lines of evidence have shown that the combination of ^{188}Re and chemotherapy or multiple dosages of ^{188}Re may increase the cytotoxic response in various cancers (*21,28,32*). It would be advantageous to design different regimes to evaluate whether ^{188}Re-liposome treatment can eradicate NSCLC and reach maximum therapeutic efficacy.

TABLE 3
Kaplan–Meier Survival Curve in Orthotopic Human NSCLC–Bearing Mice

Parameter	^{188}Re-BMEDA	^{188}Re-liposome
Sample size (*n*)	9	9
Median survival (d)	26	40

P = 0.0045; 95% confidence interval, 0.1131–0.9615. Plot is shown in Figure 6D.

CONCLUSION

The current results demonstrate that PEGylated ^{188}Re-liposome can effectively suppress the growth of human NSCLC and extend the average life span of tumor-bearing mice. This radiopharmaceutical was taken up by NSCLC in vivo, but direct imaging of its accumulation in orthotopic tumor lesions may be largely dependent on tumor size. Moreover, the pharmacokinetics and dosimetry suggest that the use of PEGylated ^{188}Re-liposome on lung cancer should be safe and deserves further investigation in larger animals. To the best of our knowledge, this is the first study investigating the efficacy of PEGylated ^{188}Re-liposome on human lung cancer. It is anticipated that this novel radiopharmaceutical will be used to design strategies for lung cancer radiotherapy.

DISCLOSURE

The costs of publication of this article were defrayed in part by the payment of page charges. Therefore, and solely to indicate this fact, this article is hereby marked "advertisement" in accordance with 18 USC section 1734. This study was supported by grants NSC100-NU-E-010-002-NU and NSC101-2623-E-010-002-NU from the Institute of Nuclear Energy Research; grant NSC102-2628-B-010-012-MY3 from the National Science Council; grant NSC 102-2325-B-001-042 from the Taiwan Mouse Clinic, which is funded by the National Research Program for Biopharmaceuticals (NRPB) at the National Science Council of Taiwan; and an "Aim for the Top University Plan" grant from the Ministry of Education, National Yang-Ming University. No other potential conflict of interest relevant to this article was reported.

ACKNOWLEDGMENTS

We thank Dr. Chia-Che Tsai and Wei-Hsin Hsu for help with ^{188}Re-liposome preparation, production, and quality assurance and the Taiwan Mouse Clinic for technical support.

REFERENCES

1. Baltayiannis N, Chandrinos M, Anagnostopoulos D, et al. Lung cancer surgery: an up to date. *J Thorac Dis.* 2013;5(suppl 4):S425–S439.
2. Howington JA, Blum MG, Chang AC, Balekian AA, Murthy SC. Treatment of stage I and II non-small cell lung cancer: diagnosis and management of lung cancer, 3rd ed—American College of Chest Physicians evidence-based clinical practice guidelines. *Chest.* 2013;143(5, suppl):e278S–e313S.
3. Ramnath N, Dilling TJ, Harris LJ, et al. Treatment of stage III non-small cell lung cancer: diagnosis and management of lung cancer, 3rd ed—American College of Chest Physicians evidence-based clinical practice guidelines. *Chest.* 2013;143(5, suppl):e314S–e340S.
4. Bernstein ED, Herbert SM, Hanna NH. Chemotherapy and radiotherapy in the treatment of resectable non-small-cell lung cancer. *Ann Surg Oncol.* 2006;13: 291–301.
5. Jassem J. Combined modality treatment with chemotherapy and radiation in locally advanced non-small cell lung cancer. *Lung Cancer.* 2001;34(suppl 2): S181–S183.
6. Wheler JJ, Falchook GS, Tsimberidou AM, et al. Aberrations in the epidermal growth factor receptor gene in 958 patients with diverse advanced tumors: implications for therapy. *Ann Oncol.* 2013;24:838–842.
7. Hung JC, Corlija M, Volkert WA, Holmes RA. Kinetic analysis of technetium-99m d,l-HM-PAO decomposition in aqueous media. *J Nucl Med.* 1988;29: 1568–1576.
8. Jovanović V, Konstantinovska D, Memedovic T. Determination of radiochemical purity and stability of ^{99m}Tc-diethyl HIDA. *Eur J Nucl Med.* 1981;6:375–378.
9. Kennedy CM, Pinkerton TC. Technetium carboxylate complexes: I—a review of Tc, Re and Mo carboxylate chemistry. *Int J Rad Appl Instrum [A].* 1988;39: 1159–1165.
10. Deutsch E, Libson K, Vanderheyden JL, Ketring AR, Maxon HR. The chemistry of rhenium and technetium as related to the use of isotopes of these elements in therapeutic and diagnostic nuclear medicine. *Int J Rad Appl Instrum B.* 1986; 13:465–477.
11. Wang HY, Lin WY, Chen MC, et al. Inhibitory effects of rhenium-188-labeled Herceptin on prostate cancer cell growth: a possible radioimmunotherapy to prostate carcinoma. *Int J Radiat Biol.* 2013;89:346–355.
12. Zhang H, Tian M, Li S, Liu J, Tanada S, Endo K. Rhenium-188-HEDP therapy for the palliation of pain due to osseous metastases in lung cancer patients. *Cancer Biother Radiopharm.* 2003;18:719–726.
13. Scheffler J, Derejko M, Bandurski T, Romanowicz G. Application of rhenium-188 HEDP in bone metastases therapy. *Nucl Med Rev Cent East Eur.* 2003;6: 55–57.
14. Rhodes BA, Lambert CR, Marek MJ, Knapp FF Jr, Harvey EB. Re-188 labelled antibodies. *Appl Radiat Isot.* Jan 1996;47:7–14.
15. Chen LC, Wu YH, Liu IH, et al. Pharmacokinetics, dosimetry and comparative efficacy of ^{188}Re-liposome and 5-FU in a CT26-luc lung-metastatic mice model. *Nucl Med Biol.* 2012;39:35–43.
16. Jeong JM, Chung JK. Therapy with ^{188}Re-labeled radiopharmaceuticals: an overview of promising results from initial clinical trials. *Cancer Biother Radiopharm.* 2003;18:707–717.
17. Edelman MJ, Clamon G, Kahn D, Magram M, Lister-James J, Line BR. Targeted radiopharmaceutical therapy for advanced lung cancer: phase I trial of rhenium Re188 P2045, a somatostatin analog. *J Thorac Oncol.* 2009;4:1550–1554.
18. Cyr JE, Pearson DA, Wilson DM, et al. Somatostatin receptor-binding peptides suitable for tumor radiotherapy with Re-188 or Re-186: chemistry and initial biological studies. *J Med Chem.* 2007;50:1354–1364.
19. Lin LT, Chiou SH, Lee TW, et al. A comparative study of primary and recurrent human glioblastoma multiforme using the small animal imaging and molecular expressive profiles. *Mol Imaging Biol.* 2013;15:262–272.
20. Euhus DM, Hudd C, LaRegina MC, Johnson FE. Tumor measurement in the nude mouse. *J Surg Oncol.* 1986;31:229–234.
21. Chang YJ, Chang CH, Yu CY, et al. Therapeutic efficacy and microSPECT/CT imaging of ^{188}Re-DXR-liposome in a C26 murine colon carcinoma solid tumor model. *Nucl Med Biol.* 2010;37:95–104.
22. Chang YJ, Chang CH, Chang TJ, et al. Biodistribution, pharmacokinetics and microSPECT/CT imaging of ^{188}Re-bMEDA-liposome in a C26 murine colon carcinoma solid tumor animal model. *Anticancer Res.* 2007;27:2217–2225.
23. Wang SJ, Lin WY, Chen MN, et al. Radiolabelling of Lipiodol with generator-produced ^{188}Re for hepatic tumor therapy. *Appl Radiat Isot.* 1996;47:267–271.
24. Howell RW, Wessels BW, Loevinger R, et al. The MIRD perspective 1999. Medical Internal Radiation Dose Committee. *J Nucl Med.* 1999;40(suppl):3S–10S.
25. Stabin MG, Sparks RB, Crowe E. OLINDA/EXM: the second-generation personal computer software for internal dose assessment in nuclear medicine. *J Nucl Med.* 2005;46:1023–1027.
26. Chan PC, Wu CY, Chang WY, et al. Evaluation of F-18-labeled 5-iodocytidine (^{18}F-FIAC) as a new potential positron emission tomography probe for herpes simplex virus type 1 thymidine kinase imaging. *Nucl Med Biol.* 2011;38:987–995.
27. Bao A, Goins B, Klipper R, Negrete G, Phillips WT. Direct ^{99m}Tc labeling of pegylated liposomal doxorubicin (Doxil) for pharmacokinetic and non-invasive imaging studies. *J Pharmacol Exp Ther.* 2004;308:419–425.
28. Chen LC, Chang CH, Yu CY, et al. Pharmacokinetics, micro-SPECT/CT imaging and therapeutic efficacy of ^{188}Re-DXR-liposome in C26 colon carcinoma ascites mice model. *Nucl Med Biol.* 2008;35:883–893.
29. Lawrence TS, Robertson JM, Anscher MS, Jirtle RL, Ensminger WD, Fajardo LF. Hepatic toxicity resulting from cancer treatment. *Int J Radiat Oncol Biol Phys.* 1995;31:1237–1248.
30. Hall EJ, Giaccia AJ. *Radiobiology for the Radiologist.* 7th ed. Philadelphia, PA: Wolters Kluwer Health/Lippincott Williams & Wilkins; 2012.
31. Tsai CC, Chang CH, Chen LC, et al. Biodistribution and pharmacokinetics of ^{188}Re-liposomes and their comparative therapeutic efficacy with 5-fluorouracil in C26 colonic peritoneal carcinomatosis mice. *Int J Nanomedicine.* 2011;6:2607–2619.
32. van Dodewaard-de Jong JM, de Klerk JM, Bloemendal HJ, et al. A phase I study of combined docetaxel and repeated high activity ^{186}Re-HEDP in castration-resistant prostate cancer (CRPC) metastatic to bone (the TAXIUM trial). *Eur J Nucl Med Mol Imaging.* 2011;38:1990–1998.